



# Triton-alpha radiative capture reaction at astrophysical energies

M. Khoddam<sup>1</sup> · H. Sadeghi<sup>1</sup> · A. Rahmani<sup>1</sup>

Received: 7 October 2023 / Accepted: 5 November 2023 / Published online: 10 November 2023  
© The Author(s), under exclusive licence to Springer Nature B.V. 2023

## Abstract

The pion-less effective field theory has been used to study the  ${}^3\text{H}(\alpha, \gamma){}^7\text{Li}$  reaction using the Faddeev equation procedure. This reaction is the seventh interaction in the Big Bang Nucleosynthesis (BBN) model which has a golden role in the estimating of  ${}^7\text{Li}$  abundance in the universe, and answering the “cosmological lithium problem”. In this work the astrophysical s-factor of the  ${}^3\text{H}(\alpha, \gamma){}^7\text{Li}$  reaction has been calculated in leading order (LO), considering the Coulomb interactions, for the dominant electrical  $E_1$  transition from the s-and p-wave initial states to the final ground state of  ${}^7\text{Li}$ , at the astrophysical range of  $E \leq 1.5$  MeV.

**Keywords**  ${}^3\text{H}$ -Alpha radiative capture · Effective field theory · Faddeev integral equations · Astrophysical s-factor

## 1 Introduction

The Big Bang nucleosynthesis model, which is one of the triple evidence for the Big Bang model, has always been considered the origin of nuclear synthesis in the world. This model includes several nuclear interactions that begin with the combination of a proton and a neutron and the production of a deuteron, leading to the production of heavier nuclei. Some of these interactions are radiation capture reactions, which are among the most important processes in nuclear synthesis. Three interactions of BBN processes are  $(\alpha, \gamma)$  radiative capture reactions.  $d(\alpha, \gamma){}^6\text{Li}$ ,  ${}^3\text{He}(\alpha, \gamma){}^7\text{Be}$ , and  ${}^3\text{H}(\alpha, \gamma){}^7\text{Li}$ , in which an alpha particle fuses with another light nucleus and produces a heavier nucleus and an electromagnetic beam. In these interactions, the electromagnetic transition takes place from an initial scattering state to a final bound or excited state. The  $(d + \alpha)$  process is the only process producing  ${}^6\text{Li}$  in the BBN model, and  ${}^7\text{Li}$  is obtained directly from the  $({}^3\text{H} + \alpha)$  reaction (10 percent) and indirectly from the interaction  $({}^3\text{He} + \alpha)$  reaction (90 percent). The importance of these processes in lithium production is that, although there is a good agreement between the values obtained from observations and calculations for the initial synthesis of  ${}^2\text{H}$  and  ${}^4\text{He}$  in the BBN

model, the prediction of this model for the  ${}^6\text{Li}/{}^7\text{Li}$  have a difference of factor 3 with Physical observations, which is called “primordial lithium problem”, and has not been reduced by nuclear experiments or new observations. This issue is considered one of the active fields in nuclear astrophysics research, the answer to this problem can open the way for many questions in nuclear astrophysics. For example, the formation of low-mass stars, the possibility of finding heavy elements in stars, cosmic rays, supernovae, etc.

The  $(\alpha, \gamma)$  processes have been studied many times with different methods and in different energy ranges to help solve the primordial lithium problem. The  $(d + \alpha)$  process that occurs in BBN in the energy range  $0.05\text{ MeV} \leq E \leq 0.4$  MeV was noticed by Robertson et al. (1984), and later by other groups and methods. Experimentally, it has recently been tested in the LUNA accelerator at the energy of 400 keV, and the results have been published in Anders et al. (2014). The study of  $({}^3\text{He} + \alpha)$  reaction was also started in 1984 by Osborne et al. (1984) with the prompt gamma experimental method, and by Filippone et al. (1983) with the theoretical method of the microscopic potential model, and later by various experimental groups such as Nara Singh et al. (2004), Confortola et al. (2007), ... and recently by Szűcs et al. (2019), as well as various theoretical methods. The  ${}^3\text{H}(\alpha, \gamma){}^7\text{Li}$  reaction, is usually studied accompanied by the  ${}^3\text{He}(\alpha, \gamma){}^7\text{Be}$  reaction, because  $({}^3\text{He}, {}^3\text{H})$  and  $({}^7\text{Be}, {}^7\text{Li})$  are mirror nuclei. Another reason is that both reactions, directly  $({}^3\text{H}(\alpha, \gamma){}^7\text{Li})$  and indirectly  $({}^3\text{He}(\alpha, \gamma){}^7\text{Be}(e^-, \nu){}^7\text{Li})$  are the producers of primordial  ${}^7\text{Li}$  with ratios of about 10 and 90 percent.

✉ M. Khoddam  
khoddam.nml@gmail.com

<sup>1</sup> Department of Physics, Faculty of Science, Arak University, Arak 8349-8-38156, Iran

This reaction was studied experimentally by Griffiths et al. (1961) since 1960 and followed by various research groups such as Schroder et al. (1987), Burzynsky et al. (1978), Brune et al. (1994), Tokimoto et al. (2001). This reaction has been investigated by various theoretical methods. The quasi microscopic phenomenological method Nollett et al. (2000). Fermionic molecular dynamics model (FMD) by Neff (2011). The M3Y potential model by Sadeghi et al. (2014b). The realistic Argonne  $V_{18}$  two-nucleon and Urbana IX Sadeghi (2013). No-core shell model with continuum (NCSMC) by Dohet-Eraly et al. (2016). The versions of the resonating group model (RGM) Soloviyev et al. (2014). And modified two-body potential model Tursunov et al. (2020).

In addition to the mentioned theoretical methods, the effective field theory (EFT) method has also been used many times for BBN interactions as a phenomenological model-independent method, which is described based on renormalization group (RG), and has been used for the systems with two and three-nucleon also for heavier nuclei. Systems like the third interaction from the BBN processes,  $(d + p)$  that was studied in 2005 by the EFT method by Sadeghi et al. (2005). The fourth reaction  $(d + d)$ , was investigated by Sadeghi et al. (2014a). Also, among  $(\alpha, \gamma)$  interactions, EFT is used during the years 2020 to 2022, to calculate all the observables related to the  $(d + \alpha)$  interaction, Nahidinezhad et al. (2020a,b, 2021, 2022). Recently, the  $(^3\text{He} + \alpha)$  radiative capture reaction has been studied by EFT and the astrophysical s-factor and the reaction rate have been calculated in astrophysical energies for two-and three-body states up to NLO, Khoddam et al. (2022a,b, 2023a,b,c).

In this work, in continuation of the study of  $(\alpha, \gamma)$  interactions, the EFT method has been used to calculate the cross-section and the astrophysical s-factor of the  $(^3\text{H}(\alpha, \gamma)^7\text{Li})$  reaction in  $E_1$  and  $E_2$  transition from the  $2S_{1/2}$ ,  $2P_{1/2}$  and  $3S_1$  initial scattering states to the  $2P_{3/2}$  ground state of  $^7\text{Li}$ . In this way, the Faddeev equation formalism has been used to obtain the numerical results.

In this paper, we begin by introducing the  $^3\text{H}-\alpha$  reaction and discuss the nuclei participating in this process. Then we present the Lagrangian of the system in the third section. The Faddeev equation method will be introduced in the fourth section along with the Faddeev integral equations and diagrams related to the  $^3\text{H}-\alpha$  reaction. The numerical findings of the astrophysical s-factor considering the Coulomb interactions in LO are presented in the next section, along with figures and tables. In the final section, a summary and conclusion are presented.

## 2 Interaction

The  $^3\text{H}(\alpha, \gamma)^7\text{Li}$  reaction, which is the seventh process (see Fig. 1) in the Big Bang nucleosynthesis processes, is a direct radiation capture process which has an important role

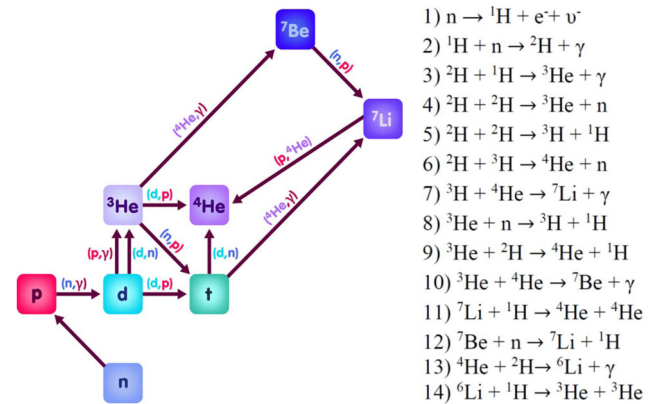


Fig. 1 Big Bang Nucleosynthesis reactions

in nucleosynthesis in stars, also in estimating the amount of primordial  $^7\text{Li}$  and solving the primordial lithium problem. This reaction with the  $Q_m = 2.465$  MeV, has been observed in the energy range of  $E_\alpha = 0.5 - 1.9$  MeV to produce  $^7\text{Li}$  in the ground state ( $^7\text{Li}(0)$ ) and in the excited state ( $^7\text{Li}^*(0.48)$ ) with a ratio of 5 : 2 Khatri et al. (2011). In this process, the electromagnetic transition is possible from the s-wave initial scattering to the final ground state at low energies ( $E \leq 0.5 \text{ MeV}$ ) and from the d-wave initial states at intermediate energies ( $0.5 \leq E \leq 1 \text{ MeV}$ ), through the  $E_1$  transition as a dominant transition. While the transition from the initial p-wave scattering states to the final ground state, in the energies of the resonance region and close to 3 MeV, is done through the  $E_2$  transition and the magnetic transition  $M_1$  is more suppressed in all energies Tursunov et al. (2019). This reaction takes place from the fusion of  $^4\text{He}$  and  $^3\text{H}$  light nuclei.

$^3\text{H}$  is the nucleus of a rare and radioactive isotope of hydrogen, which has two neutrons and one proton. The half-life of this isotope is 12.32 years, which is considered the heaviest isotope of hydrogen and its formation is through interactions such as  $^2\text{H}(^2\text{H}, p)^3\text{H}$ . Triton has  $J^\pi = 1/2^+$  and its decay mode is  $\beta^-$ . Its binding energy is  $E_B = 8.4818$  MeV, with this amount of energy the triton nucleus is decomposed into all its components. The energy of a neutron separation from this nucleus is equal to  $S_n = -6.2572$  MeV, with this amount of energy, the triton nucleus is split into a neutron and a deuteron nucleus.

The  $^4\text{He}$  nucleus is the most stable isotope of helium with  $J^\pi = 0^+$  and the binding energy and mass of 27.2436 MeV and 3728.4 MeV respectively.

From the fusion of these two light nuclei in a direct radiation capture process, a  $^7\text{Li}$  nucleus and  $\gamma$  electromagnetic radiation are produced.  $^7\text{Li}$  isotope with a mass of 7.016 MeV is the most abundant isotope of lithium (92.41 percent). This nucleus with 4 neutrons and 3 protons and isospin 1/2 is considered the mirror nucleus of  $^7\text{Be}$ , that  $n \leftrightarrow p$  transformation is done through a  $\beta^\pm$  decay which

can not change the nuclear energy. This nucleus can be seen in the ground state with  $J^\pi = 3/2^-$  or in the excited state with  $E = 0.478$  MeV and  $J^\pi = 1/2^-$ , that this excited state returns to the ground state in  $0.9 \pm 0.1 \times 10^{-13}$  by emitting a gamma ray. At low energy ( $E \leq 1.5$  MeV), our working range, usually in the formation of the  ${}^3H(\alpha, \gamma){}^7Li$  process, we can ignore the internal structure of the alpha particle, and consider it as a point particle, because the excitation energy of the alpha particle is much higher than the range we are working on. Also, considering a cluster structure consisting of deuteron and neutron for triton, the  ${}^3H + \alpha$  reaction can be done through the three channels; an elastic reaction between the pair of  $(dn)$  and an alpha particle as an observer. Neutron exchange process between the pair of  $(n\alpha)$  and a deuteron as a spectator. And the deuteron exchange reaction between the  $(d\alpha)$  pair and a neutron as an observer.

### 3 Effective Lagrangian

In the study of a low-energy system described by effective field theory, Lagrangian includes two parts: kinetic energy and interaction energy, and several coupling constants, which represent the strength of an interaction. These constants are usually calculated phenomenologically and with the help of experimental data. The Leading Order (LO) Lagrangian of the  ${}^3H(\alpha, \gamma){}^7Li$  reaction ( $\mathcal{L} = \mathcal{L}_1 + \mathcal{L}_2$ ) consists of one-body terms,  $\mathcal{L}_1$ , including the kinetic energy of alpha, deuteron, and neutron single particles, and two-body terms,  $\mathcal{L}_2$ , including the kinetic energy of  $(dn)$ ,  $(n\alpha)$  and  $(d\alpha)$  two-bodies, as well as the sentences describing the interaction between the constituent particles of the pairs.

$$\begin{aligned} \mathcal{L}_1 = & \mathcal{N}^\dagger \{i v \cdot D + \frac{1}{2m_n} [(v \cdot D)^2 - D^2]\} \mathcal{N} \\ & + d^\dagger \{i v \cdot D + \frac{1}{2m_d} [(v \cdot D)^2 - D^2]\} d \\ & + \mathcal{A}^\dagger \{i v \cdot D + \frac{1}{2m_\alpha} [(v \cdot D)^2 - D^2]\} \mathcal{A}, \end{aligned} \quad (1)$$

where  $(\mathcal{N}, m_n)$ ,  $(d, m_d)$  and  $(\mathcal{A}, m_\alpha)$  describe the field and mass of the neutron, deuteron in the spin singlet state, and alpha, respectively.  $v$  refers to the velocity vector with the condition of  $v^2 = 1$ , and  $D$  is the covariant derivative.

The two-body part of the Lagrangian is defined as;

$$\begin{aligned} \mathcal{L}_2 = & \sigma_0 t^\dagger \{i v \cdot D + \frac{1}{2(m_n + m_d)} [(v \cdot D)^2 - D^2] - \Delta_0\} t \\ & + \sigma_1 h^\dagger \{i v \cdot D + \frac{1}{2(m_\alpha + m_d)} [(v \cdot D)^2 - D^2] - \Delta_1\} h \\ & + \sigma_2 p^\dagger \{i v \cdot D + \frac{1}{2(m_\alpha + m_n)} [(v \cdot D)^2 - D^2] - \Delta_2\} p \end{aligned}$$

$$\begin{aligned} & + y_0 [t^\dagger (C_0 d \overleftrightarrow{\partial}_a N) + h.c.] \\ & + y_1 [h^\dagger (C_1 N \overleftrightarrow{\partial}_b A) + h.c.] \\ & + y_2 [p^\dagger (C_2 d \overleftrightarrow{\partial}_c A) + h.c.]. \end{aligned} \quad (2)$$

In two-body part,  $\sigma_i$ , ( $i = 0, 1, 2$ ) describes the sign factor.  $t$ ,  $h$  and  $p$  are the two-body fields of  $(dn)$ ,  $(d\alpha)$  and  $(n\alpha)$ .  $y_i$ , ( $i = 0, 1, 2$ ) defines the coupling constants for the two-body vertices.  $\overleftrightarrow{\partial} \dots$ , represents the Galilean invariant derivative defined as;  $\overleftrightarrow{\partial} \dots = [\frac{\vec{m} \cdot \vec{\nabla} - \overleftarrow{m} \cdot \overleftarrow{\nabla}}{\vec{m} + \overleftarrow{m}}] \dots$  where  $\vec{m}$  ( $\overleftarrow{m}$ ) is the mass of acting field with  $\vec{\nabla}$  ( $\overleftarrow{\nabla}$ ) operators.  $C_i$ , ( $i = 0, 1, 2$ ) is Clebsch-Gordan coefficient.

Here the coupling constants are defined as follows;

$$y_0^2 = \frac{8\pi}{\mu_{nd}^2 r^{(2s_{1/2})}}, y_1^2 = \frac{8\pi}{\mu_{n\alpha}^2 r^{(2p_{1/2})}}, y_2^2 = \frac{8\pi}{\mu_{d\alpha}^2 r^{(3s_1)}}. \quad (3)$$

Also, the  $\Delta_i$ , ( $i = 0, 1, 2$ ) operators described the corrections in kinetic energy and defined as;

$$\begin{aligned} \Delta_0 &= \frac{2}{\mu_{(nd)} r^{(2s_{1/2})}} (\frac{1}{a^{(2s_{1/2})}} - \mu), \\ \Delta_1 &= \frac{2}{\mu_{(n\alpha)} r^{(2p_{1/2})}} (\frac{1}{a^{(2p_{1/2})}} - \mu), \\ \Delta_2 &= \frac{2}{\mu_{(d\alpha)} r^{(3s_1)}} (\frac{1}{a^{(3s_1)}} - \mu), \end{aligned} \quad (4)$$

$\mu$  refers to the renormalization scale.

We can define the alpha, nucleon, and dimeron propagators ignoring the Coulomb interaction for one-body section of the Lagrangian as follows;

$$iS_{\mathcal{A}}(p_0, P) = \frac{i}{p_0 - \frac{p^2}{2m_\alpha} + i\varepsilon}. \quad (5)$$

$$iS_{\mathcal{N}}(p_0, P)_{\alpha\beta}^{ab} = \frac{i\delta_{\alpha\beta}\delta_{ab}}{p_0 - \frac{p^2}{2m_N} + i\varepsilon}. \quad (6)$$

$$iD_{ij}(p_0, P) = \frac{i\delta_{ij}}{p_0 - \frac{p^2}{4m_N} - \Delta_I + i\varepsilon}. \quad (7)$$

The main idea of effective field theory is to make a theory in the desired momentum scale. The selection of this scale is done according to the conditions of the problem and based on the degrees of freedom of the system, to take the problem out of the infinite state, and to separate the unimportant details from the problem. Usually, two momentum scales are chosen; a high momentum scale,  $M_{hi}$  (breakdown scale), and a low momentum scale,  $M_{lo}$ , which includes the typical momentum of the system.

After writing the Lagrangian, depending on which channel the interaction takes place, we can write the general formula for the effective range expansion (ERE), Eq. (8). Then we can rewrite it for the desired channel, in this way, the

scattering length and the inverse of the effective range, will be equal to the low momentum scale,  $Q$ , and high momentum scale,  $\Lambda$ , respectively.

$$k^{2l+1} \cot \delta_l = -\frac{1}{a_l} + \frac{r_l}{2} k^2 - \frac{\mathcal{P}_l}{4} k^4 + \dots, \quad (8)$$

where  $a_l$  and  $r_l$  are the scattering length and effective range, and  $\mathcal{P}_l$  describes the shape parameter in the  $l_{th}$  partial wave. Also,  $k$ ,  $\delta$ , and  $l$  represent the momentum, phase shift, and the arbitrary angular momentum respectively. Usually, low energy observables are expanded with an approximate schema in terms of  $\frac{M_{lo}}{M_{hi}} \sim \frac{Q}{\Lambda} \ll 1$ , and we can arrange the power counting rules for each process according to the powers of  $Q$ , in each contribution, and make a ranking schema as  $(\frac{M_{lo}}{M_{hi}})^n \sim (\frac{Q}{\Lambda})^n$ , which are used to estimate accurate and correctable errors. For example in the KSW procedure, the leading order (LO) of the perturbation expansion is equal to  $(n = 0)$ , and the higher orders are obtained from  $(n = 1)$  for Next to leading order (NLO),  $(n = 2)$  for next to next to leading order ( $N^2LO$ ), and  $\dots$ . The LO has the largest contribution and the next levels have smaller contributions respectively. In pion-less EFT, the high momentum scale, is in the order of pion mass,  $M_{hi} = \Lambda = 140$  MeV, and  $M_{lo} = Q = \sqrt{m_N B_d} \sim 45$  MeV.

#### 4 Faddeev integral equation

The Faddeev equation formulation is considered one of the most common methods in solving three-body quantum mechanics problems, which can be used to write integral equations for possible channels in an interaction, and the pairs and observers of each channel as follows;

$$\mathcal{F}_i(q) = \sum_{j \neq i} 4\pi \int_0^\Lambda q'^2 dq' \mathcal{X}_{ij}(q, q'; E) \tau_j(q'; E) \mathcal{F}_j(q') \quad (9)$$

In this equation, index  $i$  refers to the spectator in each channel and  $j$  is the exchange particle's index,  $\Lambda$  represents the ultraviolet cutoff which is equal to the high momentum scale of the system in pion-less EFT.  $\tau_j$  functions are the two-body matrices, and  $X_{ij}$  defines the kernel functions. The following relations describe two-body matrices and kernel functions, respectively.

$$\begin{aligned} \tau_i(q; E) &= \tau_{jk}(E - \frac{q^2}{2\mu_{i(jk)}}), \\ \tau_{jk}(E) &= \frac{1}{4\pi^2 \mu_{jk}} \gamma_1(k^2 - k_R^2). \end{aligned} \quad (10)$$

$\mu_{i(jk)}$ ,  $q$ ,  $E$  are the reduced mass of three bodies, Jacobian momentum, and the three-body binding energy, respectively.

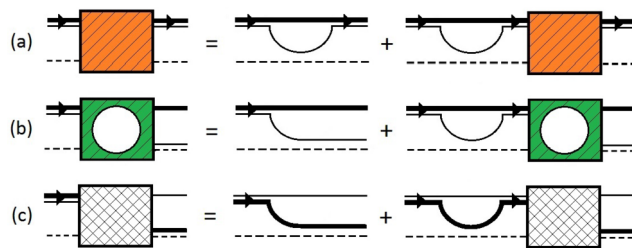


**Fig. 2** Feynman diagrams of the amplitude associated with elastic scattering channels, neutron, and deuteron exchanges at LO, considering Coulomb effects. The thick line and the thin line represent the deuteron propagator and the neutron field respectively, and the dashed line represents alpha. Solid dashed cubic depict the amplitudes of  $^3H$  and  $\alpha$  in the elastic scattering channel. Hollow and white dashed cubics represent the amplitudes of  $^3H$  and  $\alpha$  in the neutron and deuteron transfer channels, respectively

$$\text{And } k = \sqrt{2\mu E}, k_R = \sqrt{\frac{1}{a_0 r_0}}.$$

$$\begin{aligned} \mathcal{X}_{ij}(q, q'; E) &= \iint p^2 dp p'^2 dp' g_{li}(p) G_0^{(i)}(p, q; E) \\ &\times g_{lj}(p') \quad i < p, q; \Omega_i \mid p', q'; \Omega_j > j, \end{aligned} \quad (11)$$

$g_{li}(p)$  and  $g_{lj}(p')$  are the form factors,  $G_0^{(i)}(p, q, E)$  is the three-body Green functions which is defined as,  $G_0^{(i)}(p, q, E) = (E - \frac{p^2}{2\mu_{ij}} - \frac{q^2}{2\mu_{i(jk)}})^{-1}$ . And  $i < p, q, \Omega_i \mid p', q', \Omega_j > j$  describes the projection of free Hamiltonian eigenstate in the partition of projector  $i$  to the free eigenstate in the partition of projector  $j$  Ji et al. (2014), which should be calculated for  $\alpha$ ,  $d$  and  $n$  spectators in various channels. How to calculate the kernel functions and Faddeev equations are presented fully for the mirror reaction in Khoddam et al. (2022a).

As we mentioned above, in this work we have used the Faddeev equation method to obtain the numerical results. Since we have considered three interaction channels; elastic scattering, and neutron and deuteron exchange channels, as  $(\alpha, dn)$ ,  $(d, n\alpha)$  and  $(n, d\alpha)$  for the  $^3H(\alpha, \gamma)^7Li$  reaction, which corresponds to the transition from the  $2S_{1/2}$ ,  $2P_{1/2}$  and  $3S_1$  initial states to the final  $2P_{3/2}$  ground state, we can write the Faddeev equation for them in the general form of;

$$\begin{aligned} \mathcal{F}_i(q) &= 4\pi \int_0^\Lambda q'^2 dq' \mathcal{X}_{ij}(q, q'; E) \tau_j(q'; E) \mathcal{F}_j(q') \\ &+ 4\pi \int_0^\Lambda q'^2 dq' \mathcal{X}_{ik}(q, q'; E) \tau_k(q'; E) \mathcal{F}_k(q'), \end{aligned} \quad (12)$$

where the  $i$ ,  $j$ , and  $k$  cyclic indices are correspond to the  $n$ ,  $d$ , and  $\alpha$ . So we can set up three Faddeev equations, and their corresponding Feynman diagrams in LO are shown in Fig. 2. In the interaction of charged particles at low energies, Coulomb scattering takes place through  $p - p$  Coulomb interactions, which is along with photon exchange. In the  $(^3H + \alpha)$  reaction, which includes three parts: input, middle, and output (scattering), Coulomb corrections are entered in



the middle part of the interaction. The effect of Coulomb interactions on the Faddeev equations requires the effect of the Coulomb propagator in these equations. Which is defined as follows,

$$i\mathcal{D}_{s(pp)}(E - \frac{3q^2}{4m_p}) = \frac{4\pi}{m_p g_s^2} \frac{-i}{(-\frac{4\pi \Delta_{s(pp)}^R}{m_p g_s^2} - 2kH(\eta))}, \quad (13)$$

where  $y_s$  is the coupling constant of the s-wave state for two protons scattering,  $k = \eta p'$ ,  $p' = \sqrt{\frac{3}{4}q^2 - m_p E - i\epsilon}$ ,  $H(\eta) = \psi(i\eta) + \frac{1}{2i\eta} - \ln(i\eta)$ ,  $\eta$  refers to the Sommerfeld parameter,  $\psi(i\eta)$  represents the logarithmic derivative of the gamma function, and  $\Delta_{s(pp)}^R$  is the renormalization constant, which is related to the scattering length  $a_c$  and the coupling constant  $y_s$  as follow;

$$\frac{1}{a_c} = \frac{4\pi \Delta_{s(pp)}^R}{m_N y_s^2} + \mu - 2k[1 - \gamma_E + \ln(\frac{\mu}{4k})] \quad (14)$$

where  $\gamma_E = 0.577215$  is the Euler's constant. The dibaryon propagator for the  $p-p$  channel in the presence of Coulomb interactions is shown in Fig. 3. The effect of the Coulomb propagator on the Faddeev equations in the ( $d\alpha$ ) channel in LO is as follows,

$$\begin{aligned} \mathcal{F}_i(q) = & 4\pi \int_0^\Lambda q'^2 dq' \mathcal{D}_{s(pp)} [4\pi \int_0^\Lambda q''^2 dq'' \mathcal{X}'_{ij}(q, q''); E) \\ & \times \tau_j(q''); E) \mathcal{X}'_{ji}(q'', q'; E) \tau_i(q'; E) \\ & + 4\pi \int_0^\Lambda q'^2 dq' \mathcal{D}_{s(pp)} [4\pi \int_0^\Lambda q''^2 dq'' \mathcal{X}'_{jk}(q, q''); E) \\ & \times \tau_k(q''); E) \mathcal{X}'_{kj}(q'', q'; E) \tau_k(q'; E) \\ & + 4\pi \int_0^\Lambda q'^2 dq' \mathcal{D}_{s(pp)} [4\pi \int_0^\Lambda q''^2 dq'' \mathcal{X}'_{ki}(q, q''); E) \\ & \times \tau_i(q''); E) \mathcal{X}'_{ik}(q'', q'; E) \tau_j(q'; E), \quad (15) \end{aligned}$$

Because interaction is a radiative capture process where capturing occurs through an electromagnetic interaction. Therefore, in the calculation of radiation capture amplitude, using effective field theory, in addition to strong interactions, photon interactions are also included in Lagrangian through minimum subtraction,  $\partial_\mu \rightarrow D_\mu = \partial_\mu + ie\hat{Q}A_\mu$ . To include the electromagnetic interactions, it is necessary to replace the derivative operators of the Lagrangian with the  $D = \vec{\nabla} - ie\vec{A}Q$  invariant derivatives and  $D_0 = \partial_0 + ieA_0Q$  time derivatives Chen et al. (1999). where  $Q$  is the electric charge operator which acts on various charged particle fields and gives different eigenvalues.  $e = \sqrt{4\pi\alpha}$  and  $\alpha = \frac{1}{137.036}$  refers to the fine structure constant. The photonic part of the Lagrangian at LO is written as follows,

$$\begin{aligned} \mathcal{L}_{photo} = & \frac{\mathcal{N}^\dagger \mathcal{N} e Q_{(3H)}}{2m_{(3H)}} [\vec{P}_{(3H)} + \vec{P}'_{(3H)}] \vec{\epsilon}_\gamma^* \\ & + \frac{\mathcal{N}^\dagger \mathcal{N} e Q_\alpha}{2m_\alpha} [\vec{P}_\alpha + \vec{P}'_\alpha] \vec{\epsilon}_\gamma^* \quad (16) \end{aligned}$$

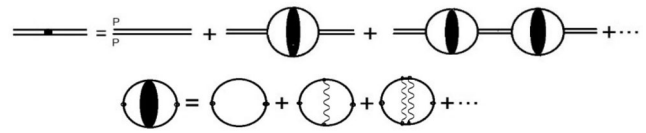


Fig. 3 Dressed dibaryon  $p-p$  propagator. The shaded ovals depict the Green's function of two nucleons along with Coulomb interaction

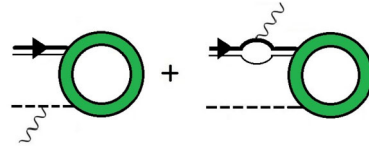


Fig. 4 Diagrams correspond to the photon part of the  ${}^3H-\alpha$  radiative capture reaction. The wavy lines define the real photons, and the rest of the symbols are similar to the Fig. 2

where  $\mathcal{N}$  is the field of charged nucleons participating in the Coulomb interaction and  $\vec{\epsilon}_\gamma^*$  represents the polarization of the emitted photon.  $Q_\alpha = 2$  and  $Q_{(3H)} = 1$  describe the charge of alpha particles and  ${}^3H$  and  $\vec{P}$ ,  $\vec{P}'$  are their input and output momenta in the  ${}^3H - \text{photon} - {}^3H$  and  $\alpha - \text{photon} - \alpha$  vertices. The corresponding diagrams are presented in the first and second lines of Fig. 4, respectively.

In this work, our goal is to calculate the astrophysical s-factor. The astrophysical s-factor is a quantity that simplifies the extrapolation and analysis of data than the cross-section because it is less energy dependent than the cross-section. So it shows a smoother plot at low energies. To calculate it, we can use the following relation.

$$S(E) = E \sigma(E) \exp(2\pi\eta), \quad (17)$$

where  $E$  describes the energy of the alpha particle in the center of the mass system.  $\eta$  is the dimensionless Sommerfeld parameter which is define as,  $\eta = z_1 z_2 \alpha \sqrt{\frac{\mu}{2E}}$ .  $z_1$  and  $z_2$  are the  ${}^3H$  and  $\alpha$  electric charges,  $\mu$  is the  ${}^3H$  and  $\alpha$  two-body reduced mass,  $\alpha$  is the finite structure constant. And  $\sigma(E)$  describes the cross section with the following definition.

$$\sigma = \frac{1}{f} \frac{q}{(1 + \frac{q}{\mu})} \Sigma_{L,S,J_i,J_f} \frac{1}{(2J_f + 1)} |\mathcal{E}_l^{L,S,J_i,J_f}|^2, \quad (18)$$

$f = \frac{v_{rel}}{8\pi\alpha}$ , and  $v_{rel}$  is the  ${}^3H$  and  $\alpha$  relative velocity.  $L$ ,  $S$ ,  $J_i$ ,  $J_f$  are the quantum numbers related to each channel. And  $|\mathcal{E}_l^{L,S,J_i,J_f}|^2$  introduces the scattering amplitude as follow,

$$|\mathcal{E}_l^{L,S,J_i,J_f}|^2 = \left(\frac{1}{3} \mathcal{F}_\alpha\right)^2 + \left(\frac{1}{3} \mathcal{F}_p\right)^2 + \left(\frac{1}{3} \mathcal{F}_d\right)^2. \quad (19)$$

After calculating the kernel functions and Faddeev equations, we must first calculate the scattering amplitude and

the cross-section according to the above relations, and finally calculate the s-factor.

## 5 Result and discussion

The study of  $(\alpha, \gamma)$  reactions is very important from both theoretical and experimental points of view, because these processes play a role as basic interactions in the development of low-mass stars like the Sun, and are also important processes in the Big Bang nucleosynthesis. One of these interactions, which, in addition to the above reasons, is particularly important due to the production of  ${}^7\text{Li}$  and helping to solve the primordial lithium problem, is the  ${}^3\text{H}(\alpha, \gamma){}^7\text{Li}$  process. Usually, at low energies, it is very difficult to measure the contribution of  $E_1$  and  $E_2$  transitions due to the low flux of virtual photons resulting from transitions  $E_1$  and  $E_2$  in this interaction and the Coulomb repulsive between the charged particles. Therefore, many theoretical methods have been invented to solve such problems. The effective field theory method, which is a phenomenological and model-independent procedure, in addition to simplifying the calculations, has good accuracy due to the possibility of correcting the results by increasing the order of the calculations. This method can provide the possibility of investigating the  $(\alpha, \gamma)$  radiation capture reactions in stellar energies with a many-body approach.

In this work, the astrophysical s-factor has been calculated for the  $E_1$  transition from the initial scattering states of  $2S_{1/2}$ ,  $2P_{1/2}$  and  $3S_1$  to the final  $2P_{3/2}$  ground state, considering the effect of Coulomb interactions as a correction in the cross-section, using the pion-less EFT method and Faddeev equations formalism, at the energies of  $E \leq 1.5$  MeV. In the process of calculations, the masses of  $m_n = 939.5654$  MeV,  $m_d = 1876.14$  MeV, and  $m_\alpha = 3727.3$  MeV is used for the particles participating in the initial channels, and the mass and binding energy of  $m({}^7\text{Li}) = 7.016$  MeV and  $E({}^7\text{Li}) = 6566.616$  MeV for the product of interaction.

As we mentioned above, we have considered three possible channels for the  ${}^3\text{H}(\alpha, \gamma){}^7\text{Li}$  reaction.  $(\alpha, dn)$  elastic scattering, and  $(d, n\alpha)$ ,  $(n, d\alpha)$  exchanging channels. In this section, the results of the calculation of the astrophysical s-factor for the  $E_1$  transition in LO with Coulomb interactions at the energy range of  $E \leq 1.5$  MeV are presented in table 1 and Fig. 5 in comparison with the results of other theoretical and experimental works.

Comparing the results of our calculation results with the EFT method shows similarities with the results of other works. The highest agreement can be seen with the experimental results of Brune et al. (1994) (with a difference of less than 5 percent), Griffiths et al. (1961), Burzynsky et al. (1978), and Tokimoto et al. (2001) in the energy range of  $E \leq 1$  MeV. In  $E \leq 0.4$  MeV there is a close similarity

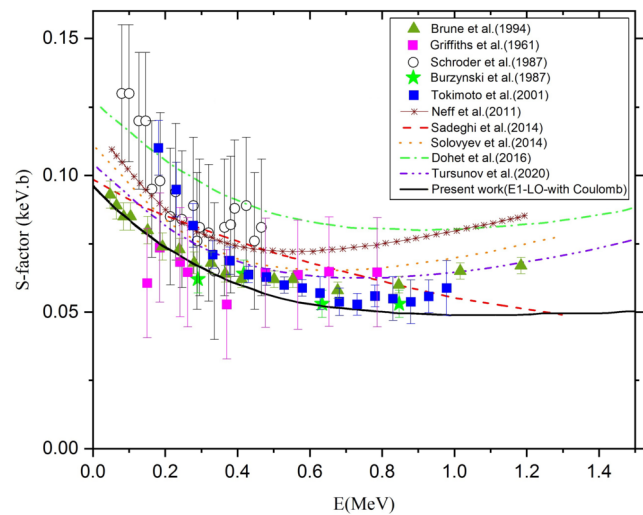


**Fig. 5** Comparison of the s-factor results in (keV.b) in LO considering Coulomb interactions at  $E_\alpha \leq 1.5$  MeV, with other available experimental data of Brune et al. (1994), Griffiths et al. (1961), Schroder et al. (1987), Burzynsky et al. (1978), Tokimoto et al. (2001) and the theoretical calculations of Neff (2011), Sadeghi et al. (2014b), Dohet-Eraly et al. (2016), Solov'yev et al. (2014), Tursunov et al. (2020)

with the experimental data of Brune et al. (1994) and Griffiths et al. (1961). In  $E \leq 0.3$  MeV there are at least eight agreement points with the data of them. Especially in the points of  $E = 0.065$  MeV,  $E = 0.085$  MeV,  $E = 0.104$  MeV,  $E = 0.185$  MeV,  $E = 0.192$  MeV and  $E = 0.280$  MeV. Which two complete matches are seen, in the point of  $S(E = 0.085) = 0.085$  keV.b with Brune et al. (1994)'s data, and with the data of Brune et al. (1994) and Griffiths et al. (1961) in  $S(E = 0.185) = 0.074$  keV.b. In the range of  $E \leq 0.4$  MeV, there is also a very close point with the data of Schroder et al. (1987) in the  $E = 0.336$  MeV. In the range of  $0.4 \leq E \leq 1$  MeV, at least three very close points can be seen with the experimental data of Brune et al. (1994), Tokimoto et al. (2001) and Burzynsky et al. (1978), particularly in the energy of  $E = 0.634$  MeV with Burzynsky et al. (1978)'s data, and in the  $E = 0.678, 0.728$  MeV with Tokimoto et al. (2001) results.

From the comparison with the theoretical results, it can be seen that our data are closer to the Tursunov et al. (2020) data by the modified two-body potential method, with an error of less than 10 percent. There is also a point of agreement in  $S(E = 1.260) = 0.049$  keV.b with Sadeghi et al. (2014b) theoretical data with the M3Y potential technique.

## 6 Summary and conclusions

One of the most important  $(\alpha, \gamma)$  interactions in Big Bang nucleosynthesis is the  ${}^3\text{H}(\alpha, \gamma){}^7\text{Li}$  reaction. The significance of this process is in the estimation of the amount of primordial  ${}^7\text{Li}$  and the rate of  ${}^6\text{Li}/{}^7\text{Li}$  to solve the lithium

**Table 1** Comparison of the s-factor values for the present work (PW) in (keV.b) in LO considering Coulomb interactions at  $E_\alpha \leq 1.5$  MeV, with other available experimental data (Exp.) from references Brune et al. (1994)(A), Griffiths et al. (1961)(B), Schroder et al. (1987)(C),

Burzynsky et al. (1978)(D), Tokimoto et al. (2001)(E) and the theoretical (Th.) calculations from references Neff (2011)(F), Sadeghi (2013)(G), Dohet-Eraly et al. (2016)(H), Soloviyev et al. (2014)(I), Tur-sunov et al. (2020)(J)

| $E_\alpha$<br>(MeV) | $S(A)$<br><i>Exp.</i> | $S(B)$<br><i>Exp.</i> | $S(C)$<br><i>Exp.</i> | $S(D)$<br><i>Exp.</i> | $S(E)$<br><i>Exp.</i> | $S(F)$<br><i>Th.</i> | $S(G)$<br><i>Th.</i> | $S(H)$<br><i>Th.</i> | $S(I)$<br><i>Th.</i> | $S(J)$<br><i>Th.</i> | $S(PW)$<br><i>(Th.)</i> |
|---------------------|-----------------------|-----------------------|-----------------------|-----------------------|-----------------------|----------------------|----------------------|----------------------|----------------------|----------------------|-------------------------|
| 0.047               | 0.093                 | –                     | –                     | –                     | –                     | –                    | 0.095                | 0.121                | 0.104                | 0.098                | 0.090                   |
| 0.065               | 0.089                 | –                     | –                     | –                     | –                     | 0.107                | 0.093                | 0.120                | 0.101                | 0.096                | 0.087                   |
| 0.085               | 0.085                 | –                     | 0.130                 | –                     | –                     | 0.100                | 0.091                | 0.115                | 0.098                | 0.094                | 0.085                   |
| 0.104               | 0.085                 | –                     | –                     | –                     | –                     | –                    | 0.091                | 0.115                | 0.096                | 0.092                | 0.083                   |
| 0.151               | 0.080                 | 0.060                 | –                     | –                     | –                     | 0.093                | 0.087                | 0.110                | 0.089                | 0.086                | 0.078                   |
| 0.185               | 0.074                 | 0.074                 | 0.098                 | –                     | –                     | 0.089                | 0.086                | 0.107                | 0.085                | 0.082                | 0.074                   |
| 0.280               | 0.068                 | –                     | –                     | –                     | –                     | 0.080                | 0.081                | 0.099                | 0.076                | 0.075                | 0.067                   |
| 0.336               | –                     | –                     | 0.065                 | –                     | –                     | 0.076                | 0.079                | 0.094                | 0.072                | 0.071                | 0.064                   |
| 0.417               | 0.064                 | –                     | –                     | 0.064                 | –                     | 0.073                | 0.075                | 0.089                | 0.069                | 0.067                | 0.059                   |
| 0.501               | 0.062                 | –                     | –                     | –                     | –                     | 0.072                | 0.071                | 0.085                | 0.066                | 0.065                | 0.055                   |
| 0.634               | –                     | –                     | –                     | 0.053                 | 0.057                 | 0.072                | 0.066                | 0.082                | 0.065                | 0.063                | 0.052                   |
| 0.678               | –                     | –                     | –                     | –                     | 0.054                 | 0.072                | 0.065                | 0.081                | 0.065                | 0.062                | 0.052                   |
| 0.728               | –                     | –                     | –                     | –                     | 0.053                 | 0.073                | 0.063                | 0.080                | 0.065                | 0.062                | 0.051                   |
| 0.847               | 0.060                 | –                     | –                     | 0.053                 | –                     | 0.075                | 0.060                | 0.080                | 0.067                | 0.063                | 0.049                   |

problem. In this study, we have applied the pionless effective field theory and the Faddeev equation formalism to study the  ${}^3\text{H}(\alpha, \gamma){}^7\text{Li}$  reaction in astrophysical energies. Effective field theory is a useful method to study nuclear reactions based on quantum field theory which can simplify the calculations with good accuracy because of the possibility of modifying the initial results by appending the Coulomb effects, increasing the order of calculations, and adding the three-body forces. We have calculated the astrophysical s-factor for the  $E_1$  transition at LO considering Coulomb interactions. The  $E_1$  transition is the dominant transition in low and intermediate energies, which is carried out from the  $2S_{1/2}$ ,  $2P_{1/2}$  and  $3S_1$  initial states to the  $2P_{3/2}$  final ground state in  ${}^7\text{Li}$ . As we used the Faddeev equation formalism, we have considered three possible channels for the  $({}^3\text{H} + \alpha)$  reaction and calculated the kernel functions related to the spectators in each channel, at the first step according to the procedure explained in Khoddam et al. (2022a), then we have calculated the Faddeev equations for these three observers and finally, the amplitude, cross-section and the s-factor have been obtained respectively. The results have been comprised of other experimental data and theoretical results with various techniques. An excellent agreement can be seen with the experimental data of Brune et al. (1994), Griffiths et al. (1961), Burzynsky et al. (1978) in the range of  $E \leq 1$  MeV.

**Author contributions** M.Kh. and H.S. wrote the main manuscript text and M.Kh. prepared Figs. 1–5. All authors reviewed the manuscript.

**Funding** No funding was received to assist with the preparation of this manuscript.

**Data Availability** All data generated or analyzed during this study are included in this published article.

## Declarations

**Competing interests** The authors declare no competing interests.

## References

- Anders, M., et al.: Phys. Rev. Lett. **113**, 042501 (2014)
- Brune, C.R., et al.: Phys. Rev. C **50**, 2205 (1994)
- Burzynsky, S., et al.: Nucl. Phys. A **473**, 179 (1978)
- Chen, J., et al.: Nucl. Phys. A **653**, 386–412 (1999)
- Confortola, F., et al.: Phys. Rev. C **75**, 065803 (2007)
- Dohet-Eraly, J., et al.: Phys. Lett. B **757**, 430 (2016)
- Filippone, B.W., et al.: Phys. Rev. C **28**, 2222 (1983)
- Griffiths, G.M., et al.: Can. J. Phys. **39**, 1397 (1961)
- Ji, C., et al.: Phys. Rev. C **90**, 044004 (2014)
- Khatri, R., et al.: Astron. Lett. **37**, 367–373 (2011)
- Khoddam, M., et al.: Astrophysics and space science **367**, 23 (2022a)
- Khoddam, M., et al.: Astrophysics and space science **83**, 367 (2022b)
- Khoddam, M., et al.: Iran. J. Sci. Technol. **47**, 1013–1027 (2023a)
- Khoddam, M., et al.: Pramana **97**, 91 (2023b)
- Khoddam, M., et al.: New Astron. **100**, 101971 (2023c)
- Nahidinezahad, S., et al.: New Astron. **80**, 101424 (2020a)
- Nahidinezahad, S., et al.: Astrophys. Space Sci. **4**, 365 (2020b)
- Nahidinezahad, S., et al.: New Astron. **82**, 101461 (2021)
- Nahidinezahad, S., et al.: New Astron. **91**, 101700 (2022)
- Nara Singh, B.S., et al.: Phys. Rev. Lett. **93**, 262503 (2004)
- Neff, T.: Phys. Rev. Lett. **106**, 042502 (2011)
- Nollett, K.M., et al.: Phys. Rev. D **61**, 123505 (2000)

Osborne, J.L., et al.: Nucl. Phys. A **419**, 115 (1984)  
Robertson, R.G., et al.: Phys. Rev. C **29**, 755 (1984)  
Sadeghi, H.: Chin. Phys. Lett. **30**, 10 (2013)  
Sadeghi, H., et al.: Nucl. Phys. A **753**, 291 (2005)  
Sadeghi, H., et al.: Chin. Phys. Lett. **31**, 012101 (2014a)  
Sadeghi, H., et al.: J. Korean Phys. Soc. **64**, 1654–1657 (2014b)  
Schroder, U., et al.: Phys. Lett. B **192**, 55 (1987)  
Solovye, A.S., et al.: Bull. Russ. Acad. Sci., Phys. **78**, 433 (2014)  
Szucs, T., et al.: Phys. Rev. C **99**, 055804 (2019)  
Tokimoto, Y., et al.: Phys. Rev. C **63**, 035801 (2001)  
Tursunov, E.M., et al.: Int. J. Mod. Phys. Conf. Ser. **49**, 1960014 (2019)

Tursunov, E.M., et al.: Nucl. Phys. A **1006**, 122108 (2020)

**Publisher's Note** Springer Nature remains neutral with regard to jurisdictional claims in published maps and institutional affiliations.

Springer Nature or its licensor (e.g. a society or other partner) holds exclusive rights to this article under a publishing agreement with the author(s) or other rightsholder(s); author self-archiving of the accepted manuscript version of this article is solely governed by the terms of such publishing agreement and applicable law.